

HENRY

Hydraulic Engineering Repository

Ein Service der Bundesanstalt für Wasserbau

Conference Paper, Published Version

Pagliara, Stefano; Palermo, Michele **Structural defence for plunge pool scour**

Verfügbar unter/Available at: <https://hdl.handle.net/20.500.11970/100060>

Vorgeschlagene Zitierweise/Suggested citation:

Pagliara, Stefano; Palermo, Michele (2006): Structural defence for plunge pool scour. In: Verheij, H.J.; Hoffmans, Gijs J. (Hg.): Proceedings 3rd International Conference on Scour and Erosion (ICSE-3). November 1-3, 2006, Amsterdam, The Netherlands. Gouda (NL): CURNET. S. 513-519.

Standardnutzungsbedingungen/Terms of Use:

Die Dokumente in HENRY stehen unter der Creative Commons Lizenz CC BY 4.0, sofern keine abweichenden Nutzungsbedingungen getroffen wurden. Damit ist sowohl die kommerzielle Nutzung als auch das Teilen, die Weiterbearbeitung und Speicherung erlaubt. Das Verwenden und das Bearbeiten stehen unter der Bedingung der Namensnennung. Im Einzelfall kann eine restriktivere Lizenz gelten; dann gelten abweichend von den obigen Nutzungsbedingungen die in der dort genannten Lizenz gewährten Nutzungsrechte.

Documents in HENRY are made available under the Creative Commons License CC BY 4.0, if no other license is applicable. Under CC BY 4.0 commercial use and sharing, remixing, transforming, and building upon the material of the work is permitted. In some cases a different, more restrictive license may apply; if applicable the terms of the restrictive license will be binding.



Structural defence for plunge pool scour

S. Pagliara*, M. Palermo*

* Department of Civil Engineering , Pisa, Italy

Plunge pool scour is a major topic in presence of hydraulic structures that foresees the production of jets. The scour hole is a function of several variables including the tailwater, the densimetric Froude number, the sediment granulometry, the water discharge. The maximum scour depth is of great interest in the design process. Aim of the paper is to analyze the effect of structures, inserted in the scour hole, in order to mitigate the scour geometry. About 300 tests have been carried out in the Hydraulic laboratory of the University of Pisa (Italy) in order to assess the advantages and the problems connected with the insertion of a rigid structures in the river bed. In this paper a first description of the phenomena is presented.

I. INTRODUCTION

The study of jets due to hydraulic structures is an important research topic in engineering practice. In fact, the impact of a jet on the basin downstream of the hydraulic structures can cause a scour phenomenon whose main geometrical parameters has to be foreseen in order to avoid structural instability. It was seen that the main parameters on which the scour process depends are the hydraulic characteristics of the jet, the water level in the basin downstream of the structure and the granulometric characteristics of the basin bed material.

The scour process is characterized by the formation of both a scour hole and a ridge. The phenomenon is characterized by the concomitance of three different phases: basin material disruption, formation of a vortex and deposit of material downstream of the scour hole.

When the jet stops, the basin material, which is let into suspension by the vortex, falls down and deposits in the scour hole. The dynamic configuration of the downstream face of the scour hole becomes static reducing its slope because of the ridge sliding. This occurrence puts in evidence that there are two typical configurations. The dynamic configuration is characterized by a relevant quantity of basin material which is in suspension in the vortex. Moreover, the jet pressure on the downstream face of scour hole is able to increase its natural slope, partially carrying the weight of the ridge. It means that when the jet stops, there are no dynamic forces and there is a partial ridge collapse. The phenomenon reaches its static configuration in which the slope of the downstream face of the scour hole becomes equal to the natural basin material friction slope and the suspended material deposits in the scour hole.

With these considerations it is evident that during the dynamic phase the scour hole is deeper than in the static phase [5]. This occurrence has to be taken in serious consideration in structures design. The measurements of bed profile during the dynamic phase showed that there can be also a great increase of the scour depth. Plunge

pool scour is a phenomenon which constitutes a significant structural risk.

Many Authors studied this phenomenon. Reference [1], [2] and [6], gave a contribution to understand the main hydraulic and geometrical parameters which characterize the scour mechanism. Pagliara et Al. [4] proposed an experimental formula to evaluate the dimensionless maximum scour depth $Z_m = z_m/D$ in which z_m is the maximum measured scour depth and D is the jet diameter. The following relation is valid in absence of any type of structural defence,

$$Z_m = f_1(F_d) \cdot f_2(\alpha) \cdot f_3(\beta) \cdot f_4(T_w) \cdot f_5(\sigma) \cdot f_6(F_u) \quad (1)$$

The previous relation shows that Z_m is a function of the densimetric particle Froude number (F_d), the jet impact angle (α), jet air content (β), relative tailwater depth (T_w), sediment non uniformity parameter (σ) and upstream Froude number (F_u), where $F_d = V_w/(g'd_i)^{1/2}$ with $V_w = Q_w/(\rho D_w^2/4)$ as the water velocity, $g' = [(r_s - r)/r]g$ as the reduced gravitational acceleration with the densities r_s and r of sediment and water, respectively, and d_i as the determining grain size. The significant length scale is either the conduit diameter D or the black-water jet diameter $D_w = [(4/\rho)(Q_w/V_w)]^{1/2}$. The air content β is equal to Q_A/Q_w , where Q_A and Q_w are air and jet water discharge, respectively. T_w is equal to h_0/D , where h_0 is flow depth as shown in Fig. 2; σ is equal to $(d_{84}/d_{16})^{1/2}$, in which d is the sediment size and the subscript indicates the percentage of passage across a sediment net. $F_u = V_u/(gh_0)^{1/2}$, in which V_u is the upstream velocity.

Aim of this paper is to analyze the effects of structures, inserted in the scour hole, in order to mitigate the jet scour.

II. EXPERIMENTAL SETUP

All the experiments were carried out in the same rectangular channel. This channel was 25 m long, 0.80 m wide and 0.90 m high. For the present study, the transversal section of the previous channel was divided longitudinally into two parts in order to assure the two dimensionality of the phenomenon. In fact, the model built inside the channel had a width of 0.20 m and a length of about 3 m. The channel narrowing was obtained using a vertical impermeable wood wall, which had the same height of the channel. At least the physical model built inside the channel had the following geometrical characteristics: 0.20 m wide, 3 m long and 0.90 m high. A certain quantity of granular material was put in this experimental model in order to simulate the mobile bed downstream of a dam spillways. The basin material employed in this study has the following granulometric

characteristics: $d_{84} = 11.4$ mm, $d_{16} = 9.0$ mm, $d_{90} = 11.63$ mm and $s = 1.13$.

Before starting each experiment, channel bed material was levelled in order to maintain the same fixed level. To simulate a dam spillway, a movable pipe was fixed on the channel. The extremity of this pipe could be changed in order to vary the jet section. Moreover, the pipe could slide in an iron guide in order to regulate the distance of the outlet from the water surface and could rotate in order to change the jet impact slope. Two pipe sections were employed whose diameters were 27 mm and 35 mm respectively. Some different fixed discharges ranging between 2.50 l/s and 5.65 l/s were investigated. In all the tests the impact angle was 30°. Fig. 1 shows the model used in experiments.

The channel bed was measured in some fixed points both transversally and longitudinally before starting each experiment. As to confront the results of various tests executed with different pipe diameters, let us define the dimensionless parameter T_w as h_0/D , where h_0 is the water level and D is the jet diameter, as shown in Fig. 2.

Four different values of T_w were investigated: 1, 5, 7 and 9. The water level in the channel was regulated using a gage in order to maintain the value of T_w constant during each test. To clarify the effects of protection works on the geometry of the scour due to the impact of jet four different structures were employed (i.e. *S*, *SF*, *SG10* and *SG17*). Fig. 3 shows the different used structures. Structure *S* is a 3 mm thick iron sheet; *SF* is an iron sheet on which 10 mm diameter holes were made and the percentage of vacuum is 54; *SG10* is an iron grid with 10 mm side square holes. Its percentage of vacuum is 66.8; *SG17* is an iron grid with 17 mm side square holes with a vacuum percentage of 70.



Figure 1. View of the physical model employed for the experiments.

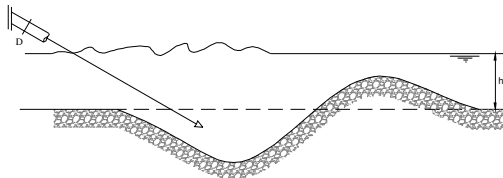


Figure 2. Definition sketch.

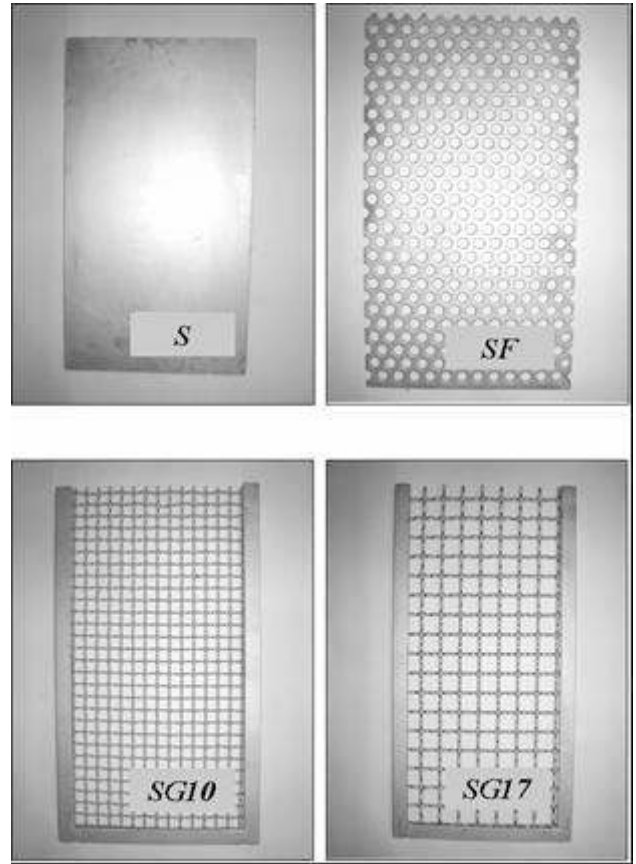


Figure 3. Scour protection structures

III. EXPERIMENTAL RESULTS

To understand the effects of the different protection works on scour mechanism, some reference tests were carried out. Namely, for each tested combination of discharge and tailwater, a reference test was carried out in order to find the longitudinal length L_0 and the maximum depth z_m , of the scour hole. These reference tests were carried out without any protection structure, as shown in Fig. 4.

Having found the reference values of L_0 and z_m , a control grid, constituted of fifteen different “control points”, was fixed in order to individuate the optimal longitudinal and vertical protection structure positions which had to be tested. For each test, according to the reference frame, the longitudinal positions were fixed in $L_0/2$, $3/4L_0$, L_0 , $5/4L_0$ and $3/2L_0$, while the three vertical positions were fixed in $+z_m/3$, 0 z_m and $-z_m/3$, as shown in Fig. 5.

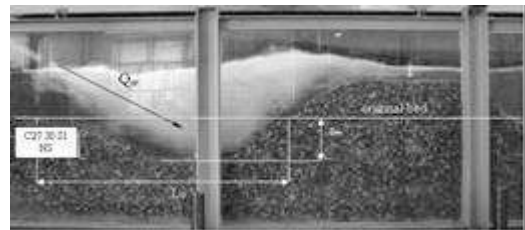


Figure 4. Example of a reference prove ($Q_w=4.50$ l/s; $T_w=7$).

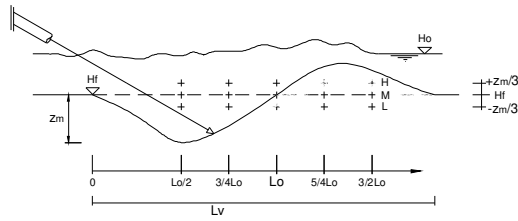


Figure 5. Control grid.

Considering all the geometrical and hydraulic parameters, a systematic investigation of all control points for each type of structure was avoided and, after having done some preliminary tests, the structures and the control positions which had to be preferred in order to minimize the scour were individuated and investigated systematically.

For each prove, including the reference one, the bed channel profile was measured at four different fixed times (1, 5, 20 and 50 minutes after the beginning of the test) in order to understand the dynamic evolution of the scour mechanism. Moreover, channel bed was measured after stopping the jet in order to analyze the final static configuration and highlight the differences with the dynamic one. The two dimensionality of the phenomenon was verified doing some transversal measurements of the maximum scour section. A thorough study of the longitudinal position $L_0/2$ was not interesting to be deepened because of the direct impact of the jet on the protection structure. In fact, for a real structure located in this position, the impact wall would be damaged by the jet energy. Moreover, for example, if a S type structure is located at $L_0/2$ and its upper upstream edge is at $+z_m/3$, a significant scour depth can be noted, as shown in Fig. 6. Fig. 7 shows that the same occurrence happens if the S type structure is located at $L_0/2$ and $-z_m/3$. The last structure settlement causes a division of the jet which directly impacts the superior part of the structure and two different vortexes are generated, one upstream and the other downstream of the structure. It means that two scour holes are present if the structure is located in this position, as shown in Fig. 7.

As also in this position the scour is deeper than in the relative reference test, this structure settlement was not considered efficient in order to minimize scour depth and this longitudinal position was not analysed further.

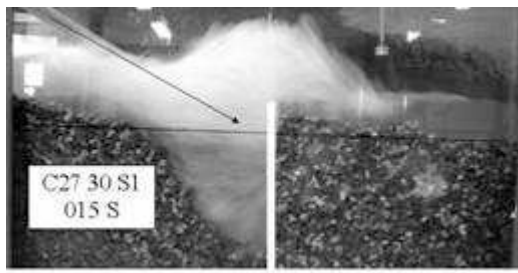


Figure 6. Scour profile in presence of S type structure located at $L_0/2$ and $+z_m/3$.

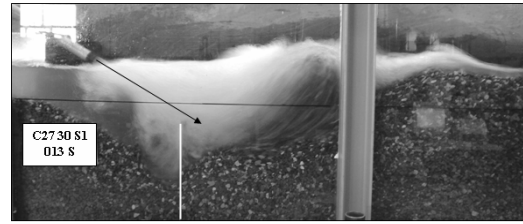


Figure 7. Scour profile in presence of S type structure located at $L_0/2$ and $-z_m/3$.

When the different structures are located at longitudinal distances ranging between $3/4L_0$ and $3/2L_0$, the jet loses a certain quantity of its energy first impacting the basin upstream of the structure. The presence of a structure, when its longitudinal position is $3/2L_0$, does not have significant effects on reducing scour depth because of the formation of a ridge downstream of the scour hole which entirely covers the structure vanishing every beneficial effect of it. Based on these considerations and on several other experimental deductions and observations, finally the positions which were considered most efficient in scour depth reduction are shown in Fig. 8 and Fig. 9 with a bold point. Fig. 8 shows the systematically investigated control positions in absence of an upstream flow, whereas Fig. 9 shows the same aspects when there is an upstream flow (Q_u) in the channel. Then they were systematically investigated further for each one of the four types of structures employed in this study.

Experimental tests, conducted with different structures, showed that one of the most important parameters which influences scour mechanism is the percentage of vacuum of the structure. Generally, maintaining constant all the other geometrical and hydraulic variables, an increase of the percentage of vacuum in the structures lets to a reduction of the scour depth. Fig. 10 shows the variables used to compare the efficiency of different structures in reducing scour depth.

z_{ms} is the maximum scour depth in presence of a protection structure, L_v is the length of the scour hole and of the ridge in the reference test, L_{vs} is the length of the scour hole and of the ridge in presence of a structure, L_0 is the length of the scour hole in the reference test, L_{0s} is the length of the scour hole in presence of a structure, h_s is the distance between water level and structure along jet direction, h_L is the distance between water level and downstream scour face along jet direction.

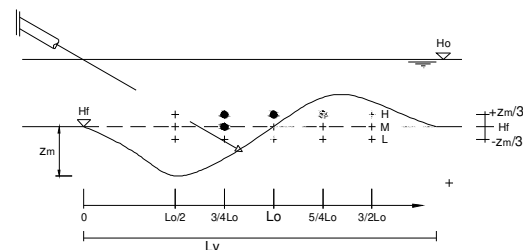


Figure 8. Systematically tested control positions in absence of an upstream channel discharge.

Fig. 11 and 12 confirm the influence of the permeability of structure on the scour mechanism and show the ratio of the maximum scour depth in presence of a protection structure to the one in absence of any type of structure. The dimensionless scour depth Z_m in absence of defence structures can be foreseen, as reported in [4], with (1) in which $f_1(F_d) = F_d$, $f_2(\alpha) = -[0.38 \cdot \sin(\alpha + 22.5^\circ)]$, $f_3(\beta) = (1 + \beta)^m$, $f_4(T_w) = [0.12 \cdot \ln(1/T_w) + C_r]/0.30$, $f_5(\sigma) = -[0.33 + 0.57\sigma]$ and $f_6(F_u) = 1 + F_u^{0.50}$, with $C_r=0.45$ for ridge presence, and $C_r=0.52$ when the ridge is artificially removed and $m = 0.75$ for the unsubmerged and $m = 0.50$ for the submerged jet configuration.

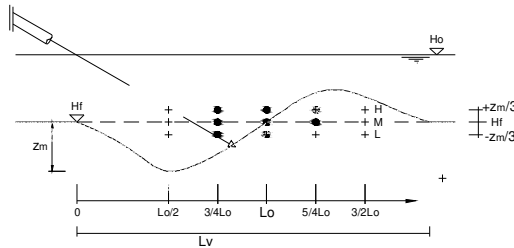


Figure 9. Systematically tested control positions in presence of an upstream channel discharge Q_u .

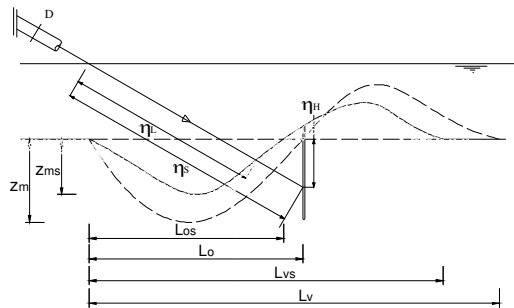


Figure 10. Schematic definition of the geometrical parameters.

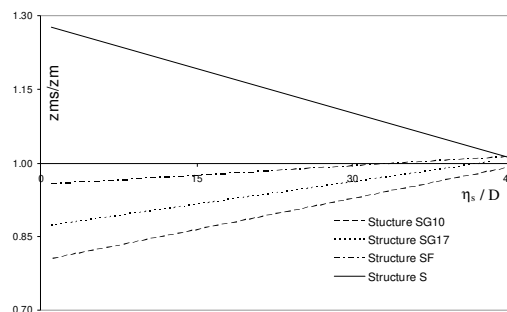


Figure 11. Comparison of the efficiency of different structures at $+z_m/3$.

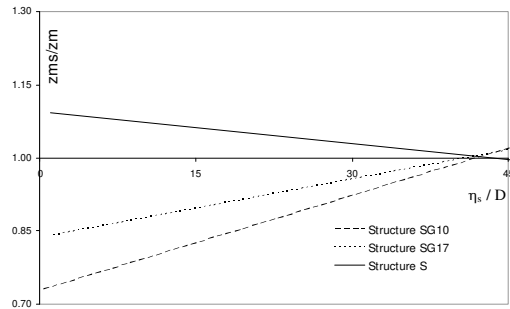


Figure 12. Comparison of the efficiency of different structure at $0z_m$.

SG10 type structure results to be the most efficient one in reducing scour depth whereas the presence of the impervious structure *S* causes an increase of the scour depth ($z_{ms}/z_m > 1$). As mentioned above, the scour reduction efficiency of the structure is generally proportional to its percentage of vacuum, but, as can be seen in the previous figures, *SG10* results to be more efficient than *SG17*. In fact, as basin material d_{90} is 11.63 mm, *SG17* allows the passage of many particles and this occurrence reduces structure efficiency.

Let us examine both the qualitative jet hydraulic behaviour and the scour mechanism that occurs in presence of the two “extreme protection structures”, *S* type and *SG10* type, respectively, whose upper upstream edge is located at $+z_m/3$. For each control position, one sketch which illustrates the phenomenon is proposed. During its path, the jet diameter increases and when it impacts the structure jet enlargement takes the shape of an “umbrella”. Scour profile remains two dimensional but jet behaviour is three dimensional. Generally, as the most relevant differences of the scour mechanism and jet behaviour are due to the variation of the structure longitudinal position, rather than the vertical one, the following sketches can be considered well representative of the qualitative phenomenon behaviour which occurs also if the upper upstream edge of structure is located both at $-z_m/3$ and $0z_m$. The only case in which there is a great difference in jet flow behaviour is when the structure is located at $L_0/2$. Especially for the *S* type structure, the vertical position influences the dynamic behaviour of the phenomenon. As shown in Fig. 13, because of the partial direct impact on the structure, the jet is divided into two parts generating two different vortices, one upstream the structure and the other one downstream. This particular flow behaviour, which is most evident in this structure configuration, is due to the imperviousness of the *S* type structure. In fact, if a *SG10* type structure is located in the same spatial configuration, there is no partial reflection of the water flow on the upstream part of structure. The permeability of the structure allows water to pass through its holes and thereby no vortex is formed on the upstream side of this structure, as shown in Fig. 14.

As mentioned above, if, in the same longitudinal position $L_0/2$, the upper upstream edge of the *S* type structure is located at $+z_m/3$, the scour profile completely changes. The jet totally and directly impacts the structure being reflected. Both vortex and scour hole are present only upstream of the structure and the jet energy dissipation causes a deep scour and the formation of two different ridges, as shown in Fig. 15. Fig. 16 shows the scour profile that occurs when a *SG10* type structure is

located at $L_0/2$ and $+z_m/3$. There is no ridge formation upstream of the structure and the scour profile is less deep than in the previous case.

This longitudinal position causes a great dissipation of energy on the structure. In practical applications it is not convenient to put a protection structure at $L_0/2$ because of the great jet impact strength that has to be opposed to dynamic forces. For this reason, this longitudinal position was not systematically investigated in the present study.

If a *S* type structure is located at $3/4L_0$ and $+z_m/3$, the jet behavior is quite similar to case in which the same structure is located at $L_0/2$ and $+z_m/3$. There is a formation of a scour hole upstream but the basin material is deposited only downstream of the structure forming a ridge, as shown in Fig. 17. This structure configuration causes the maximum observed scour depth.

The settlement of a *SG10* type structure at $3/4L_0$ and $+z_m/3$ gave interesting results. In fact, in this structure configuration there is the minimization of the scour depth. Moreover, scour volume results to be the minimum and the quantity of the material put in rotation is maximum. Fig. 18 shows scour profile and jet behavior in this configuration.

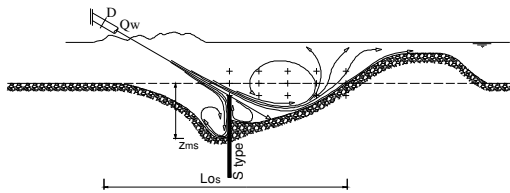


Figure 13. Qualitative scour and flow behavior in presence of a *S* type structure at $L_0/2$ and $-z_m/3$.

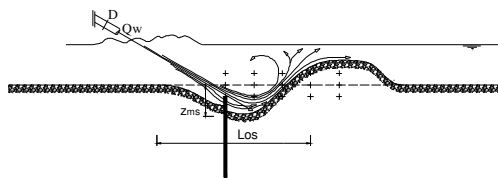


Figure 14. Qualitative scour and flow behavior in presence of a *SG10* type structure at $L_0/2$ and $-z_m/3$.

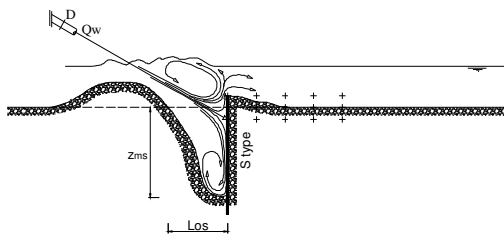


Figure 15. Qualitative scour and flow behavior in presence of a *S* type structure at $L_0/2$ and $+z_m/3$.

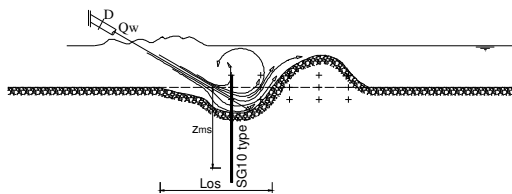


Figure 16. Qualitative scour and flow behavior in presence of a *SG10* type structure at $L_0/2$ and $+z_m/3$.

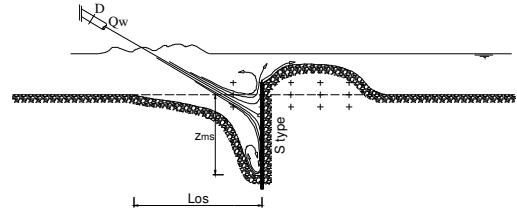


Figure 17. Qualitative scour and flow behavior in presence of a *S* type structure at $3/4L_0$ and $+z_m/3$.

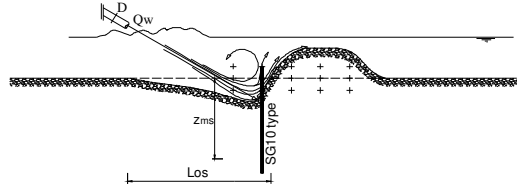


Figure 18. Qualitative scour and flow behavior in presence of a *SG10* type structure at $3/4L_0$ and $+z_m/3$.

If a *S* type structure is located at L_0 and $+z_m/3$, the maximum scour volume occurs because the jet, before reaching the structure has enough energy to put in motion a great quantity of basin material. Fig. 19 shows the scour profile that occurs in this case.

As shown in Fig. 20, the same thing happens if a *SG10* structure is located in the same spatial configuration. Moreover, through the structure holes, a certain quantity of jet air content is able to pass, reducing its erosive energy. For this reason, the basin material at the structure toe becomes more stable and the material volume put in motion by the jet flow is less than in the previous case.

When a *S* or *SG10* type structure is located at $5/4L_0$ and $+z_m/3$, the scour profile is quite similar and depends on tailwater T_w . In fact, for low tailwater values ($T_w=1$), both the structures support the ridge downstream and the solid transport does not easily pass over the structure. This occurrence obliges the basin material to remain in scour hole reducing the scour depth. Fig. 21 shows the scour profile that occurs in presence of a *S* type structure when $T_w=1$.

When both *S* and *SG10* type structures are located in the same previous spatial configuration ($5/4L_0$ and $+z_m/3$), if the tailwater increases ($T_w>1$), the jet does not impact directly the structure which is submerged by the basin material. The structure permeability does not influence the scour mechanism and scour profile tends to be similar to that one that occurs without any protection structure. Fig. 22 and Fig. 23 show the scour profiles that occur in presence of a *S* and *SG10* type structure, respectively.

When a *S* or *SG10* type structure is located at $3/2L_0$ and $+z_m/3$, the structure is practically not influential on scour mechanism and the scour profile is almost the same of the reference test, as shown in Fig. 24.

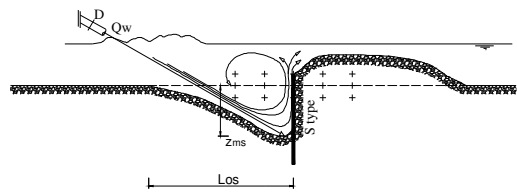


Figure 19. Qualitative scour and flow behavior in presence of a *S* type structure at L_0 and $+z_m/3$.

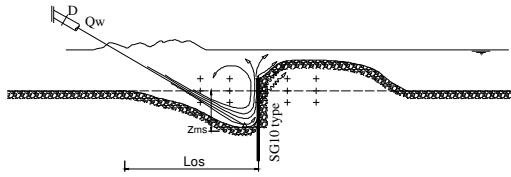


Figure 20. Qualitative scour and flow behavior in presence of a SG10 type structure at L_0 and $+z_m/3$.

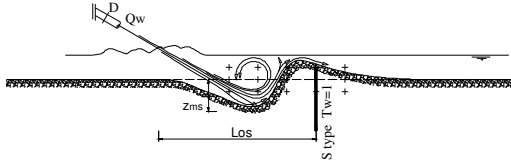


Figure 21. Qualitative scour and flow behavior in presence of a S type structure at $5/4L_0$ and $+z_m/3$ when $T_w=1$.

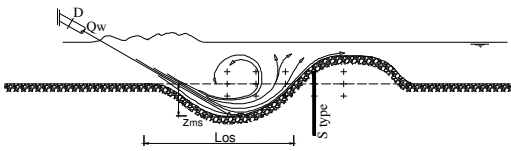


Figure 22. Qualitative scour and flow behavior in presence of a S type structure at $5/4L_0$ and $+z_m/3$ when $T_w>1$.

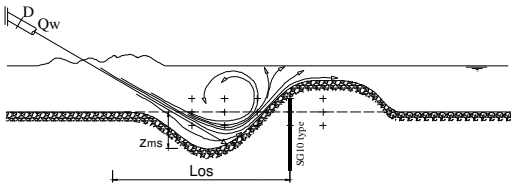


Figure 23. Qualitative scour and flow behavior in presence of a SG10 type structure at $5/4L_0$ and $+z_m/3$ when $T_w>1$.

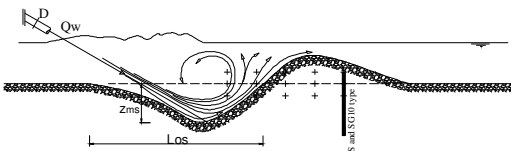


Figure 24. Qualitative scour and flow behavior in presence of both S and SG10 type structure at $3/2L_0$ and $+z_m/3$.

The previous qualitative description of different scour profiles that occur for different structure positions shows that the scour mechanism, in presence of a protection structure, is mostly influenced by the longitudinal position and permeability (percentage of vacuum) of the structure. Four different scour mechanisms and profiles can be individuated.

The scour typology called “Type 0” occurs when the presence of the structure is negligible and the scour mechanism is the same of the reference test. This scour typology typically occurs when the longitudinal position of the structure is too far from the scour hole.

The scour typology called “Type A” occurs when the jet, after hitting the structure, goes down its toe. This typology typically occurs when the structure is located

near the jet outflow and the scour depth upstream of the structure becomes maximum. This phenomenon is most evident in presence of impervious structures (S type).

The scour typologies called “Type B₁” and “Type B₂” occur when the jet does not have enough energy to reach the structure toe. The difference between these two typologies is that in the former case (Type B₁) the jet directly impacts the structure whereas in the latter (Type B₂) the jet cannot impact on the structure directly due to the formation of a ridge which covers the structure.

Fig. 25 shows the scour typology classification, where $P_s(x)$ is the dimensionless longitudinal position of the structure and I is its percentage of vacuum (permeability). No indications about vertical structure position are given in this classification. It does not mean that the vertical position of the structure does not have an influence on scour depth, but it means that the qualitative scour typology depends on the longitudinal position of the structure. The same considerations can be made for variable T_w . Figg. 26-29 show the different scour typologies that were observed in the present study.

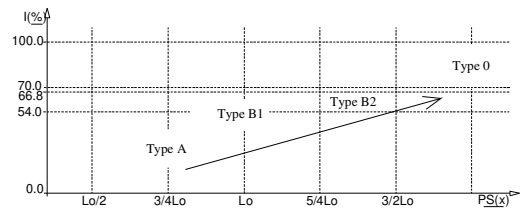


Figure 25. Scour typology classification.

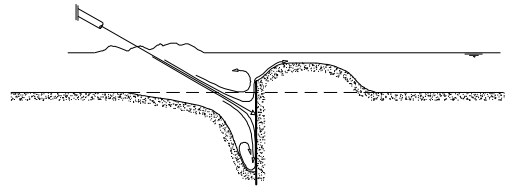


Figure 26. “Type A” typology.

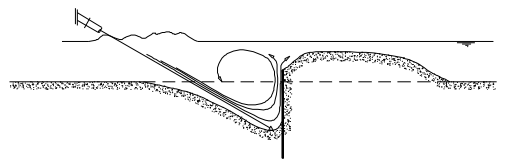


Figure 27. Type B₁ typology.

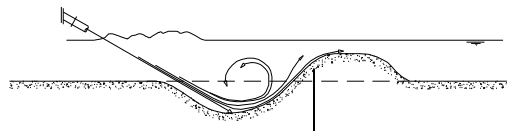


Figure 28. Type B₂ typology.

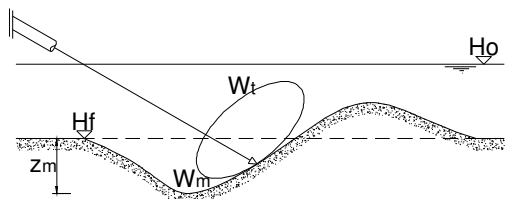


Figure 29. “Type 0” typology.

IV. CONCLUSIONS

This experimental study investigated the effects of the presence of different types of structures in order to mitigate the jet scour geometry. The parameters that were varied in order to understand their influence on the phenomenon are: jet discharge, jet diameter, tailwater T_w and selected vertical and horizontal positions of the structure. The different percentage of vacuum (permeability) of the employed structures has a significant effect on the scour mechanism. Tests in which a S type structure was employed show that the presence of this structure typology generally causes an increase of the scour depth compared to the reference test which is carried out in the same hydraulic conditions, whereas in presence of a $SG10$ type structure the scour depth is generally less. The effect of the tailwater is to reduce the jet impact energy on stilling basin. It means that an increase of the tailwater causes a reduction of the scour depth and transported bed material volume. In presence of an upstream channel discharge, with all the other parameters constant, the scour depth increases because of the removal of a certain quantity of bed material from scour hole and ridge. The maximum reduction of the scour depth and of material volume removed by jet energy was observed in presence of a $SG10$ type structure located at $3/4L_0$, whereas, in presence of a S type structure located in the same longitudinal position, the maximum scour depth was observed. A scour typology classification, depending

on I and $Ps(x)$ parameters, is proposed and it consents to classify the jet scour typology.

REFERENCES

- [1] Canepa, S. and Hager, W.H., 2003, Effect of Air Content on Plunge Pool Scour, *Journal of Hydraulic Engineering* 129(5), 358-365.
- [2] Mason, P.J., 2002, Review of Plunge Pool Rock Scour downstream of Srisaïlam Dam, Rock Scour due falling high-velocity jets, A.J. Schleiss & E. Bollaert eds Balkema: Lisse.
- [3] Minor, H.E., Hager, W.H. and Canepa, S., 2002, Does an Aerated Water Jet Reduce Plunge Pool Scour, Rock Scour due falling high-velocity jets, A.J. Schleiss & E. Bollaert eds Balkema: Lisse
- [4] Pagliara, S., Hager, W.H. and Minor, H.E., 2006, Hydraulics of Plane Plunge Pool Scour, *Journal of Hydraulic Engineering*.
- [5] Pagliara, S., Hager, W.H. and Minor, H.E., 2004, Plunge Pool Scour in Prototype and Laboratory, Conf. Hydraulics of dams and river structures, Teheran: 165-172, Balkema: Leiden.
- [6] Rajaratnam, N. and Mazurek, K.A., 2002, Erosion of a Polystyrene Bed by Obliquely Impinging Circular Turbulent Air Jets, *Journal of Hydraulic Research* 40(6), 709-716.